

Statistical Analysis of Color Differences on Iris Images for Supporting Cluster Headache Diagnosis

Inmaculada Mora-Jiménez¹^a, Andrés Iglesias-Rojano¹, Mohammed El-Yaagoubi¹^b,
José Luis Rojo-Álvarez¹^c and Juan Antonio Pareja-Grande²^d

¹Department of Signal Theory and Communications, Telematics and Computing Systems,
Rey Juan Carlos University, Madrid, Spain

²Department of Neurology, Hospital Universitario Fundación de Alcorcón, Madrid, Spain

Keywords: Iris, Color Space, Color Similarity, Cluster Headache, Histogram Matching, Cross-correlation, Kullback-Leibler Divergence, Image Analysis.

Abstract: It is well known the existence of certain headaches in humans caused by the sympathetic hypofunction, either congenital or developed at birth. These pathologies, called cluster headaches, are physically manifested by the change in texture, color and/or intensity of the iris eye on the painful side. The automatic study of these variations would make it possible to provide quantitative measures of the existence of such pathology from color images of the left and right iris of a particular individual. In this context, this work analyzes the color of the left and right irises to identify chromatic differences between the irises belonging to the same individual by analyzing three color spaces. The iris color distribution in the same eye has been studied, as well as the degree of similarity and divergence between the chromatic distributions of irises in both eyes. Cross-correlation between color feature vectors exhibited low detection capabilities, whereas a relative measure based on the Kullback-Leibler divergence provided good performance to show color differences in the irises. No color space was identified as the most appropriate for evidencing color differences in all the scrutinized cases. The results obtained are promising on a dataset with eight patients, and can be considered a proof of concept on which it is necessary to extend the analysis with a larger database. From a practical viewpoint, this characterization could help to discriminate patients who attend the neurology department suffering from headache.

1 INTRODUCTION

The iris is the colored part of the eye located between the pupil and the ciliary zone. It has a set of grooves, ridges, and pigmented regions, all of them situated within a ring bounded in the inner part by the pupil, in such a way that the light penetrating in the eye is tuned and adjusted to different environmental situations. The iris coloration is known to be produced by the concentration of melanin, which secretion depends on the sympathetic nervous system (Wielgus and Sarna, 2005). There are many factors contributing the eye color and its variation, with iris patterns being unique for each person. This uniqueness of the human iris is used in iris scans for per-

sonal identification, with lower error rates than those obtained with face and fingerprint recognition (Sangwine and Horne, 2008). This is the reason for one of the most widespread applications related with the iris being biometry, as far as the probability of two iris being similar has been estimated as 1 to 10^{72} , and also taking into account that it remains stable throughout our life. Biometric systems have been proposed from the digital segmentation and analysis of iris images, from the use of the Hough transform to Gabor filters, and local versus global image windows, among many others (e.g., see (Ma et al., 2003)).

On the other hand, the presence of abnormal iris coloration or texture has been related to some diseases. For instance, trigeminal autonomic cephalalgias belong to group III of the International Headache Society, and they share the clinical features of pain felt in the area supplied by the first division (V-1) of the trigeminal nerve (Pareja et al., 1997). Clus-

^a <https://orcid.org/0000-0003-0735-367X>

^b <https://orcid.org/0000-0003-0189-6075>

^c <https://orcid.org/0000-0003-0426-8912>

^d <https://orcid.org/0000-0002-3260-3880>

ter headache (CH) is the most usual of this kind of cephalalgias, being predominant in male with onset often in the 20s, and it is often accompanied with severe unilateral, orbital or periorbital pain, with several autonomic features. As summarized in (El-Yaagoubi et al., 2020), a sympathetic hypofunction remains latent and subclinical between attacks, but it can be shown by provocative tests with eye-drop substances. If there is a persistent but subtle and constitutional sympathetic hypofunction in the symptomatic side, the iris of that side is expected to be less pigmented, and this can likely happen during the first years after birth. Accordingly, one of the signs of CH could be different iris coloration in a patient's eyes, and this difference could be subtle and not always noticeable by simple visual inspection. These previous works propose that the screening and early detection of CH could be addressed by creating biomarkers from subtle color changes in the iris of both eyes from a given patient.

The use of machine learning techniques has been proposed for providing the clinicians with methods detecting color differences between both eyes (El-Yaagoubi et al., 2020), with promising results. An alternative way to create new biomarkers using statistical tools to characterize iris image distributions, is proposed in the present work, given the vast amount of existing methods devoted to biometry using the iris. For instance, a system was delivered in (Demirel and Anbarjafari, 2008) using color histograms as pixel statistic feature vectors for recognition of irises in order to perform cross correlation between the histogram of a given iris and those from available individuals in a database, in which the final assignment was assigned by a majority voting scheme. Specifically, our main contribution here was to scrutinize the raw statistical distributions of colors and their differences between the eyes of a given subject, using histograms of the iris color components in several color spaces and the Kullback-Leibler divergence for their comparison. This can represent a principled input feature space in machine learning systems designed to provide neurologists with biomarkers in CH.

The rest of the paper is structured as follows. First, color spaces characteristics are summarized, in particular for RGB, HSI, and CIELAB model spaces. Then, the color feature vectors are described, as well as the approaches using cross-correlation and Kullback-Leibler divergence, for their comparison. Next, the dataset used in our experiments is described, and the results of comparisons are subsequently presented. Finally, conclusions are drawn and directions for future research are highlighted.

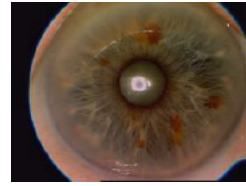


Figure 1: Color Iris image, captured with a high resolution camera (Zeiss FF 450 plus Fundus IE).

2 COLOR SPACES

Color is the way the Human Visual System (HVS) perceives radiation from part of the electromagnetic spectrum, approximately between the wavelengths of 300 nm and 830 nm (Tkalcic and Tasic, 2003). Figure 1 shows the eye image (sclera, iris and pupil) captured with a high resolution camera in the department of neurology of Hospital Universitario Fundación de Alcorcón in Spain.

In the field of Image Processing, a color model is an abstract mathematical model specifying the way in which colors can be represented as a set of numbers (González and Woods, 2007). Thus, color spaces aim to facilitate the specifications of colors in some standard way, by creating a coordinate system such that each color is mapped as a point onto it.

Some color spaces are hardware oriented (cameras, monitors, printers), while others are more adequate for color processing. In digital image processing, the RGB (red, green and blue) space is mainly used for cameras and monitors, CMY (cyan, magenta and yellow) for printers and HSI (hue, saturation and intensity) which is closer to the human eye perception, is usually convenient for image processing and analysis because it separates color and intensity information. In this line, the CIELAB space (luminosity, red-green and yellow-blue) or CIE $L^*a^*b^*$, generally called $L^*a^*b^*$, is also interesting because it separates intensity and colors in a way more similar as the HVS performs (differences in colors are uniformly perceived).

In this work, the RGB, HSI and CIELAB models have been considered.

2.1 RGB

The RGB (Red, Green, Blue) color model is a sensory model characterized by representing each color by its three primary spectral components of red (R), green (G), and blue (B) (González and Woods, 2007). This model is based on the Cartesian coordinate system, with the color gamut forming a cube, where each of the main axes quantifies the proportion of red, green

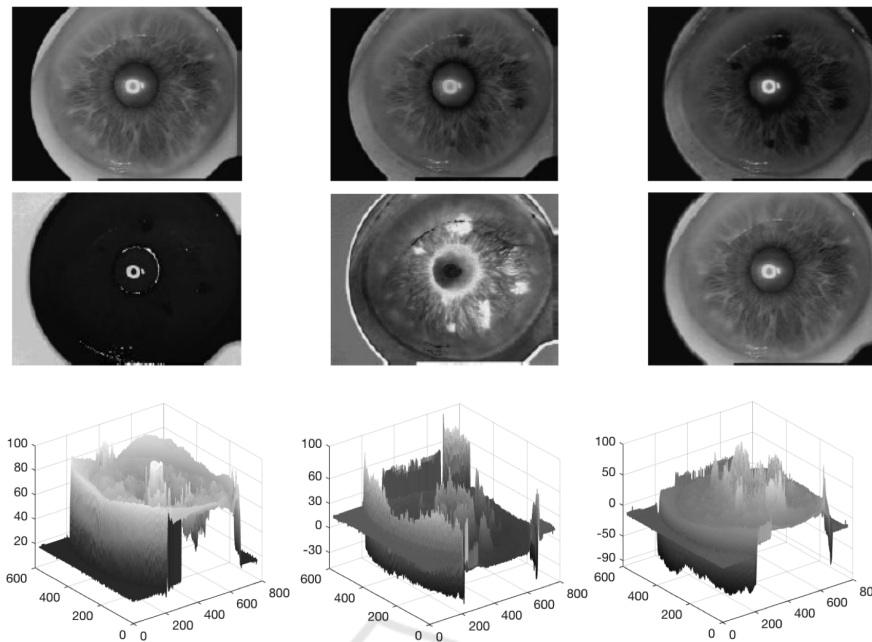


Figure 2: Color components of the image in Figure 1: upper panel (from left to right, R , G and B); middle panel (from left to right, H , S and I); lower panel (from left to right, L^* , a^* and b^*).

and blue light that has a specific color (Tkalcic and Tasic, 2003). Thus, a color RGB image can be interpreted as a collection of three monochrome images, one for each primary color. The upper panel in Figure 2 shows the R , G and B components associated with the eye image displayed in Figure 1.

It is interesting to remark that the components in the RGB color space present a high correlation between them, especially in natural images (Sangwine and Horne, 2008).

2.2 HSI

Compared to the RGB model, the HSI model provides a more intuitive description of color for humans, describing color through three components; hue (H), saturation (S) and brightness (I) (González and Woods, 2007).

The HSI model, which decouples the intensity component from the chromatic part (hue and saturation), is defined through a non-linear transformation of the RGB color space. This transformation modifies the cube subspace of the RGB model, turning it into two cones joined at their base. Geometrically, the saturation component S corresponds to the radial distance from the cone, quantifying the mixture with white light. The component H describes the dominant wavelength and is determined as the angle that the particular color point makes with respect to the angle of zero degrees (wavelength associated with a

red color). The range for H is $[0, 360)$ degrees, with an angular separation of 120 degrees between each of the primary colors R , G and B . Lastly, the intensity component I refers to the vertical axis of the cones and incorporates achromatic information, with low/high values of I corresponding to dark/light colors. In general, both S and I take values in the interval $[0, 1]$, and H is usually normalized within $[0, 1]$.

The middle panel in Figure 2 shows the H , S and I components associated with the eye image displayed in Figure 1.

2.3 CIELAB

The *Commission Internationale d'Eclairage* (CIE) is a non-profit organization devoted to publish standards related to science, technology and art in the fields of light and lighting. In 1976, the CIE proposed the CIELAB space to define a perceptually linear representation of color, characterized by representing the separation between colors proportionally to the visual differences between them.

The $L^*a^*b^*$ components are obtained by applying a set of nonlinear transformations to the RGB model (Sangwine and Horne, 2008), providing a subspace that corresponds to a sphere. The component L^* represents the brightness of the color and contains the achromatic information. The range of variation of L^* is the interval $[0, 100]$: values close to 0 represent dark colors up to black, while high values in-

dicating light colors up to white. On the other hand, the a^* and b^* components can take positive and negative values, and define a measure of the amount that certain color is magenta-green and yellow-blue, respectively. For a better visualization of the a^* and b^* components (potentially with negative values), a three-dimensional representation has been chosen in the lower panel of Figure 2 (the xy plane corresponds to the spatial coordinates of the image).

3 STATISTICAL APPROACHES FOR QUANTIFYING IRIS COLOR DIFFERENCES

There are not two identical irises, including those of twins and even the two irises of one and the same person (Juniati et al., 2020). However, we are not interested in the iris texture pattern structure, mostly determined by fibers, nerves and vessels. Instead, our goal is to identify color differences in the eyes of the same person, focusing on the global distribution of the iris color. For this purpose, we consider the color histograms (one histogram per color component) and propose two techniques to quantify their differences.

3.1 Color Feature Vectors

The histogram of a monochrome image is a bar chart representing the distribution of the pixel values in the image (González and Woods, 2007). Each bar corresponds to a group of values, determined by the width of the bar (also named bin width), while the bar height is the number of image pixels with values within the bin. Regardless of the image size, values in the histogram are normalized to represent probability estimations (calculated as relative frequencies).

Although the histogram discards information about the spatial distribution of intensity levels, it is a very useful tool in image analysis for image characterization (González and Woods, 2007). Thus, histograms allow the evaluation of image attributes such as contrast and brightness. In general, a low contrast image will have the histogram bars clustered in a narrow range, while an image with high contrast will have a balanced histogram. In image processing, histogram matching is used to transform the histogram of any image to a specific one. The histogram equalization technique is a special case in which the specified histogram is uniformly distributed. Though we also consider histogram matching, our approach is completely different, since no transformation is performed, just a quantification of the similarity between

histograms to determine their matching degree.

The basis of our work is inspired by the biometric recognition system proposed in (Demirel and Anbarjafari, 2008), where each color component of the iris image is characterized by a feature vector F obtained from the corresponding histogram. The length of F depends on the number of considered bins. In color images, a histogram is represented for each component of the color model. Color histograms in this work are computed only considering the pixels associated with the iris (manually segmented from the whole image).

Let us assume L bins in the histogram, denoted as b_0, b_1, \dots, b_{L-1} and uniformly distributed in the whole range of the corresponding color component. Considering the RGB model, three feature vectors F_R^I, F_G^I and F_B^I representing the color histograms of the image I , are obtained:

$$\begin{aligned} F_R^I &= [f_{R,b_0}^I, \dots, f_{R,b_{L-1}}^I] \\ F_G^I &= [f_{G,b_0}^I, \dots, f_{G,b_{L-1}}^I] \\ F_B^I &= [f_{B,b_0}^I, \dots, f_{B,b_{L-1}}^I] \end{aligned} \quad (1)$$

To make the iris characterization independent on the image and iris size, note that each feature vector can be normalized so that its L elements can be interpreted as probabilities.

3.2 Cross Correlation

In the signal processing field, cross-correlation allows us to measure the similarity of two series as a function of the displacement τ of one series relative to the another one (Rabiner and Gold, 1975). Thus, the statistical similarity between two images can be measured by computing the cross-correlation between the histograms of the respective images.

The authors of (Demirel and Anbarjafari, 2008) propose to use the maximum absolute value of the cross-correlation coefficient between the color histograms of a given iris and those associated with individuals in a database for iris recognition. The idea is to determine the identity of the individual as the one in the database for which the maximum value of the cross-correlation coefficient is obtained.

With a different approach, in this work we propose to calculate the cross-correlation R between two feature vectors F obtained from histograms, see Eq.(1). The feature vectors considered to compute R are associated with the same color component in each iris (left and right, I_L and I_R) of the same individual I . The mathematical formulation of cross-correlation is dependent on the shift τ between sequences F^{I_L} and F^{I_R} , as follows:

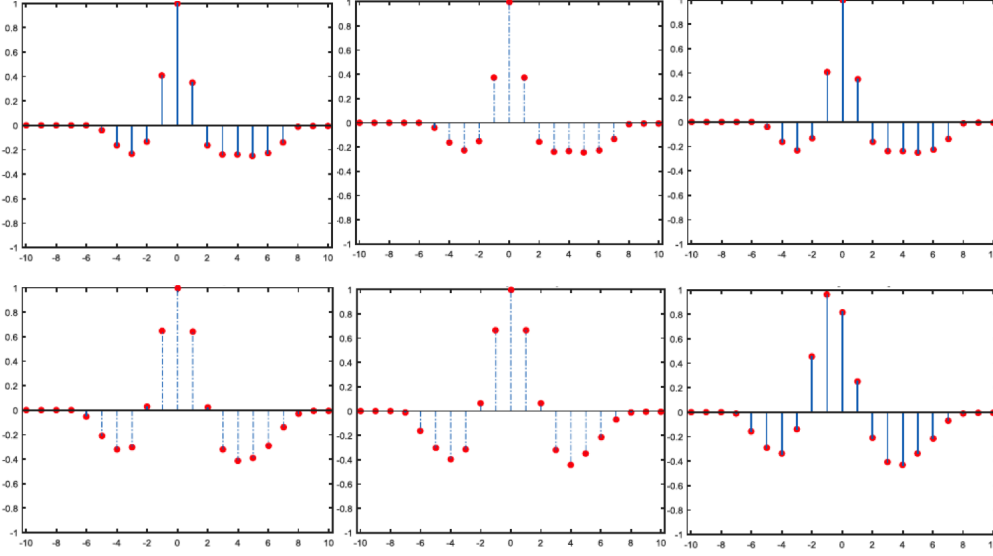


Figure 3: Average cross-correlation between feature vectors of the R component when considering the left iris (left panels), the right iris (middle panels) and the left and right iris (right panels) of two patients: healthy patient (upper panels) and patient with CH (lower panels).

$$R(\tau) = \begin{cases} \frac{\sum_{k=0}^{L+\tau-1} (f_{b_k-\tau}^{IL} - \bar{F}^{IL})(f_{b_k}^{IR} - \bar{F}^{IR})}{\sqrt{\left[\sum_{k=0}^{L-1} (f_{b_k}^{IL} - \bar{F}^{IL})^2\right] \left[\sum_{k=0}^{L-1} (f_{b_k}^{IR} - \bar{F}^{IR})^2\right]}} & \text{for } \tau < 0 \\ \frac{\sum_{k=0}^{L-\tau-1} (f_{b_k}^{IL} - \bar{F}^{IL})(f_{b_{k+\tau}}^{IR} - \bar{F}^{IR})}{\sqrt{\left[\sum_{k=0}^{L-1} (f_{b_k}^{IL} - \bar{F}^{IL})^2\right] \left[\sum_{k=0}^{L-1} (f_{b_k}^{IR} - \bar{F}^{IR})^2\right]}} & \text{for } \tau \geq 0 \end{cases} \quad (2)$$

where \bar{F}^{IL} and \bar{F}^{IR} are the average values of sequences F^{IL} and F^{IR} , respectively. The denominator in Eq. (2) has a normalization effect in the series $R(\tau)$, so that the cross-correlation values are within $[-1, 1]$. Note that $R(\tau) = 0$ indicates no correlation, while maximum correlation is obtained for $|R(\tau)| = 1$.

When considering a specific color component C , our hypothesis is that the maximum correlation value between F_C^{IL} and F_C^{IR} should be centered at $\tau=0$ (no shift). This would show a similar distribution for the C -th color component in both eyes (bin rates coincide with respect to their positions). Note that this statement would be true as long as the comparisons are made with identical bin widths and positions between the two histograms. Therefore, when calculating the maximum cross-correlation value between the eye feature vectors of a healthy patient, values close to one should be obtained at $\tau=0$. This would show that both sequences have the same structure regarding the distribution of the intensity levels in a particular color component. For the case of patients with CH, it is expected that the maximum value is obtained for $\tau \neq 0$.

For illustration, Figure 3 shows the average cross-correlation as a function of the shift τ between se-

quences. Feature vectors linked to the histogram of the R component of the two irises of the same person have been considered for two cases: a healthy patient (upper panels) and a patient diagnosed with CH (lower panels). The average is computed over four disjoint subsets of pixels in the same iris image, as detailed in Subsection 4.1. Note that the highest cross-correlation value corresponds to $\tau = 0$ when the histograms of the same iris (left or right) are considered, both for the healthy and for the patient with CH. However, when considering cross-correlation between histograms of the left and right irises, the highest cross-correlation value is located in $\tau = 0$ for the healthy patient and in $\tau = -1$ for the patient with CH. This result shows statistical differences in the distribution of the intensity levels of the red color component in the left and right irises for the patient with CH. Though only results for the R component are presented, similar outcomes are obtained when considering components G and B for these cases.

3.3 Kullback-Leibler Divergence

In contrast to cross-correlation, which measures similarity between two probability distributions linearly, the Kullback-Leibler Divergence or D_{KL} (Kullback and Leibler, 1951) provides a nonlinear measure of the difference between two distributions.

Let be P and Q two probability distributions of a discrete random variable with L possible values in b_0, \dots, b_{L-1} , the Kullback-Leibler Divergence between P and Q is defined by

$$D_{KL}(P||Q) = \sum_{i=0}^{L-1} P(b_i) \ln \left(\frac{P(b_i)}{Q(b_i)} \right) \quad (3)$$

According to this measure, the closer the value of D_{KL} is to zero, the more similar P and Q are. In our scenario, P and Q correspond to two feature vectors as those in Eq. (1).

4 EXPERIMENTS AND RESULTS

4.1 Image Dataset

A set of 16 iris images from 8 patients obtained in the Ophthalmology Department of the Hospital Universitario Fundación Alcorcón (Madrid, Spain) is available. The high-resolution camera Zeiss FF 450 plus Fundus IE, 768x576 pixels with 451 Visupac Digital version 3.2.1 digital file system was used. Images were taken under the same light conditions and exposure parameters, counteracting the effect of the flash by making the reflection on the pupil, trying not to affect the iris brightness. The neurologist JA Pareja-Grande performed the diagnosis of these patients, resulting in one healthy patient (HP), three patients who have some kind of pathology affecting the iris color but it is not confirmed that such pathology is CH (DP1, DP2 and DP3), and four individuals with confirmed diagnosis of CH (CHP1, CHP2, CHP3 and CHP4). Figure 4 and Figure 5 display the irises of each patient in the study.

The iris segmentation is manually performed by removing pupil and sclera. Subsequently, for a more robust statistical analysis, the pixels of each iris are separated into four disjoint subsets or partitions. Pixels for each partition were randomly distributed in the iris, so that the values of cross-correlation and Kullback-Leibler divergence presented in the following tables are averaged.

4.2 Use of Histogram Cross-correlation

The average cross-correlation was computed considering each component of the three color subspaces. Following the approach presented in Subsection 3.2, just the healthy patient (HP) was correctly identified by using the cross-correlation of each of the nine color components. For patients identified as CHP2, CHP3 and CHP4, the cross-correlation technique did not identify color differences in any component of the three color spaces. For the group of patients with no confirmed CH diagnosis, cross-correlation of at least one component of each color space revealed differ-

ences between both irises for two of the three patients (DP1 and DP2) in Figure 4.

After analyzing these results, we concluded that the histogram cross-correlation does not seem adequate to identify most of the patients with CH in our dataset. In fact, just the patient with the most evident differences in the iris color (CHP1) is identified.

4.3 Use of Kullback-Leibler Divergence

We present now in Table 1 the average values of D_{KL} computed when considering the same color feature vectors as those in Subsection 4.2. Each row in Table 1 is associated with a color component, and each column refers to the D_{KL} when considering probability distributions (computed from Eq. (1)) within the same eye and between both eyes of the same patient. Note that the obtained values do not seem comparable between patients: for example, the D_{KL} for the component H when considering both irises of the healthy patient takes the value 0.01731, which is higher than that associated with the component H of CHP1 (0.00384), which in principle is contrary to our hypothesis (divergence value closer to 0, more similar distributions).

Since there can also be significant differences in absolute values when comparing estimates of the mass probability function (obtained from the iris partitions) in the same iris, we propose to compute a relative measure. It is obtained by normalizing the D_{KL} when considering feature vectors of both irises with the D_{KL} obtained using feature vectors of each of the irises. The results are shown in Table 2 and Table 3, i.e. two tables to consider all patients in our dataset. As an example, the value 27.16 in the first column and first row in Table 2 is obtained as the ratio between 0.00718 and 0.00026.

From Table 2, none of the D_{KL} ratios exceeds two orders of magnitude for the case of the healthy patient (column HP). In contrast, for all patients with CH (Table 3) there is always at least one component of the three color spaces for which this ratio exceeds 100 (two orders of magnitude). For example, in the case of CHP1, the RGB color space seems to be the most suitable for identifying differences between irises, with high difference in the relative distributions between irises for the three components. The $L * a * b^*$ space seems best suited to show differences in the case of CHP2, while only the component b^* shows a ratio greater than 100 (shown in bold). For CHP4, the components H and S seem the least appropriate for showing color differences in the irises. Again, these two components offer the least relative difference for the patient DP3. It is interesting to remark that, in general, patients with CH do not show in our

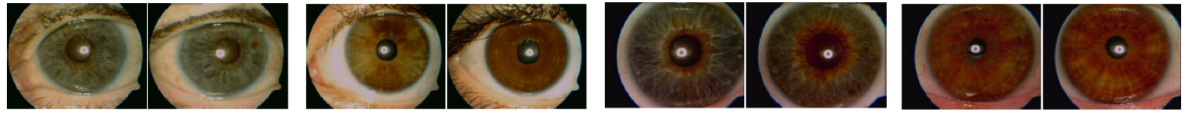


Figure 4: Left and right iris images associated with: the healthy patient (left, identified as HP) and three patients with doubt in the CH diagnosis (patients identified from right to left as DP3, DP2 and DP1).

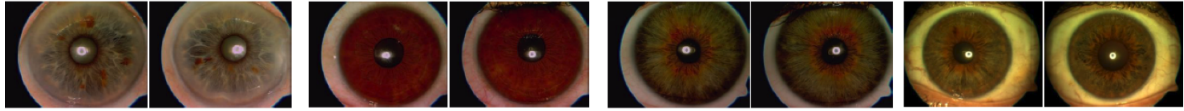


Figure 5: Left and right iris images associated with patients diagnosed with CH, named: CHP1 (left), CHP2, CHP3 and CHP4 (right).

Table 1: Average D_{KL} for each component of the RGB, HSI and $L^*a^*b^*$ spaces when three patients are considered: HP, DP1 and CHP1. For each patient, only the left iris (column labeled “Left”), only the right iris (column labeled “Right”) and both irises (column labeled “Both”) are considered.

	HP			DP1			CHP1		
	Left	Right	Both	Left	Right	Both	Left	Right	Both
<i>R</i>	0.00026	0.00059	0.00718	0.00086	0.00049	0.69376	0.00023	0.00024	0.20515
<i>G</i>	0.00036	0.00054	0.02151	0.00060	0.00067	1.58974	0.00014	0.00019	0.23238
<i>B</i>	0.00026	0.00059	0.02301	0.00039	0.00041	0.75488	0.00016	0.00019	0.26849
<i>H</i>	0.00109	0.00075	0.01731	0.00081	0.00056	0.13888	0.00044	0.00046	0.00384
<i>S</i>	0.00075	0.00084	0.05878	0.00061	0.00088	0.59718	0.00036	0.00047	0.19486
<i>I</i>	0.00084	0.00070	0.02580	0.00076	0.00071	1.24638	0.00042	0.00056	0.26411
L^*	0.00024	0.00029	0.01895	0.00026	0.00032	1.15035	0.00022	0.00018	0.22983
a^*	0.00011	0.00006	0.00172	0.00010	0.00004	0.61492	0.00001	0.00002	0.00102
b^*	0.00010	0.00019	0.00281	0.00010	0.00006	0.04871	0.00006	0.00003	0.00558

Table 2: Ratio of the average D_{KL} for each component of the RGB, HSI and $L^*a^*b^*$ spaces when four patients are considered: HP, DP1, DP2 and DP3. For each patient and color component, the column labeled “Both/Left” contains the ratio of the average D_{KL} of both irises to that of the left irises, while column labeled “Both/Right” refers to the ratio of the average D_{KL} of both irises to that of the right iris. Figures in bold indicate relative measures greater than 100.

	HP		DP1		DP2		DP3	
	Both/Left	Both/Right	Both/Left	Both/Right	Both/Left	Both/Right	Both/Left	Both/Right
<i>R</i>	27.61	12.17	806.69	1415.83	270.32	273.66	1489.91	927.85
<i>G</i>	59.75	39.83	2649.57	2372.74	702.74	654.72	139.67	109.66
<i>B</i>	88.50	39.00	1935.59	1841.17	3027.95	2813.13	145.57	91.48
<i>H</i>	15.88	23.08	171.45	248.00	287.84	251.08	29.26	21.88
<i>S</i>	78.37	69.98	978.98	678.61	1858.27	1797.27	21.73	22.11
<i>I</i>	30.71	36.85	1639.97	1755.46	516.85	561.16	351.85	169.85
L^*	78.95	65.34	4424.42	3594.84	604.06	667.40	616.42	416.77
a^*	15.63	28.67	6149.20	15373.00	2779.63	2150.27	1577.93	1110.57
b^*	28.10	14.78	487.10	811.83	3203.30	14092.98	2024.80	1589.49

(reduced) dataset the highest relative differences.

From the results, it could be concluded that intermediate values of the proposed relative measure lead to a clearer diagnosis of CH, while more pronounced color differences (see results for DP1 and DP2) might not be so closely related to the same stages of CH diagnosis, or even be related to other pathologies.

5 CONCLUSIONS AND FUTURE WORK

In this work, we have addressed the suitability of the cross-correlation series compared with the Kullback-Leibler divergence in order to provide us with quality biomarkers for cluster headache. Whereas previous efforts had been devoted to design machine learning schemes accounting for the differences in

Table 3: Ratio of the average D_{KL} for each component of the RGB, HSI and $L^*a^*b^*$ spaces when the four patients diagnosed with CH are considered. For each patient and color component, the column labeled “Both/Left” contains the ratio of the average D_{KL} of both irises to that of the left irises, while column labeled “Both/Right” refers to the ratio of the average D_{KL} of both irises to that of the right iris. Figures in bold indicate relative measures greater than 100.

	CHP1		CHP2		CHP3		CHP4	
	Both/Left	Both/Right	Both/Left	Both/Right	Both/Left	Both/Right	Both/Left	Both/Right
<i>R</i>	891.95	854.79	384.47	355.80	20.01	21.03	575.23	306.46
<i>G</i>	1659.85	1223.05	235.53	115.95	24.80	21.25	1178.46	768.58
<i>B</i>	1678.06	1413.10	78.81	54.22	52.96	16.93	221.62	179.19
<i>H</i>	8.72	8.34	1351.64	267.01	29.01	28.05	28.18	43.88
<i>S</i>	541.27	414.59	136.11	98.56	20.50	18.61	83.89	96.73
<i>I</i>	628.83	471.62	545.83	525.34	17.53	23.45	654.68	418.55
L^*	1044.68	1276.83	1135.23	401.34	17.36	35.80	1370.98	999.81
a^*	102.00	51.00	692.14	454.07	8.43	12.84	135.49	196.85
b^*	93.00	186.00	1048.50	518.60	135.27	222.59	984.58	1059.58

color of a given patient with direct representation of color neighborhood of each pixel, here we focused on building principled features based on color space histograms.

Our results show that the difference between iris coloration can be detected in terms of both luminance and chrominance, as the color resulting from melanin concentration is also dependent of brightness. In addition, cross-correlation based schemes seem to exhibit low detection capabilities, whereas the relative measure based on the Kullback-Leibler Divergence seems to provide us with good results. That is, the proposed procedure based on D_{KL} provides moderate fluctuations in healthy subjects, yielding increased fluctuations in some (or even all) components of the color spaces in the case of patients with CH.

The most evident limitation of our study is the reduced number of iris images, which also include patients with doubted diagnostic of CH. It is interesting to remark that assembling this kind of images represents an additional workload for clinicians and hospital staff. In this sense, the present work evidences that digital signal processing could provide us with suitable biomarkers for CH diagnosis and their use in the clinical environment.

ACKNOWLEDGEMENTS

This work has been partly supported by the Spanish Research Project PID2019-106623RB-C41.

REFERENCES

Demirel, H. and Anbarjafari, G. (2008). Iris recognition system using combined histogram statistics. In

Proceedings of the 23rd International Symposium on Computer and Information. IEEE.

El-Yaagoubi, M., Mora-Jiménez, I., Jabrane, Y., Muñoz-Romero, S., Rojo-Álvarez, J., and Pareja-Grande, J. (2020). Quantitative cluster headache analysis for neurological diagnosis support using statistical classification. *Information*, 11(393):1–13.

González, R. and Woods, R. (2007). *Digital Image Processing*. Pearson Prentice Hall, 3rd edition.

Juniati, D., Budayasa, I., and Khotimah, C. (2020). The similarity of iris between twins and its effect on iris recognition using box counting. *Communications in Mathematical Biology and Neuroscience*, (90):1–13.

Kullback, S. and Leibler, R. (1951). On information and sufficiency. *Annals of Mathematical Statistics*, 22(1):79–86.

Ma, L., Tan, T., Wang, Y., and Zhang, D. (2003). Personal identification based on iris texture analysis. *IEEE Trans Pat An Mach Intel*, 25:1519–33.

Pareja, J., Espejo, M., Trigo, M., and Sjaastad, O. (1997). Congenital horners syndrome and ipsilateral headache. *Funct. Neurol.*, 12:123–31.

Rabiner, L. and Gold, B. (1975). *Theory and Application of Digital Signal Processing*. Prentice Hall.

Sangwine, S. and Horne, R. (2008). *The Colour Image Processing Handbook*, chapter 4, pages 67–90. Chapman and Hall.

Tkalcic, M. and Tasic, J. (2003). Colour spaces: Perceptual, historical and applicational background. In *The Region 8 EUROCON 2003. Computer as a Tool*. IEEE.

Wielgus, A. and Sarna, T. (2005). Melanin in human irides of different color and age of donors. *Pigment Cell Res.*, 18:454–64.